Int. J. Electrochem. Sci., 14 **(2019)** 8709 – 8719, doi: 10.20964/2019.09.32

International Journal of
ELECTROCHEMICAL
SCIENCE
www.electrochemsci.org

Investigation of Pb-Sr and Pb-Ca Binary Alloys as Grids for Lead-Acid Batteries

Zhongfei Wu[1,#], Chen Hu[2,#], Juyi Mu[2], Zhaoqin Sun[2], Ruirui Zhao[1,3,], Hongyu Chen[1,3,*]*

[1] School of Chemistry and Environment, South China Normal University, Guangzhou, Guangdong, 510006, China
[2] State Key Laboratory of Operation and Control of Renewable Energy & Storage Systems, China Electric Power Research Institute, Beijing, 100192, China
[3] Base of Production, Education & Research on Energy Storage and Power Battery of Guangdong Higher Education Institutes, Guangzhou, Guangdong, 510006, China
[*]E-mail: zhaoruirui@m.scnu.edu.cn; hychen@scnu.edu.cn
[#]These authors contribute equal to this work

Received: 2 May 2019 / *Accepted:* 21 June 2019 / *Published:* 31 July 2019

The grid is one of the most important components in lead-acid configuration, thus searching suitable alloys to meet the requirement of the grid is vital and urgent. Considering the similar chemical properties of Sr to Ca, we employed Sr element as a new dopant into the lead matrix, and the detailed properties of this novel binary Pb-Sr alloys are studied. Combining the results from hydrogen/oxygen evolution reaction (HER/OER) study, anti-corrosion investigations under constant potential or current, it can be concluded that this new dopant is not suitable to be used as a sole additive to the grid for a lead-acid battery. The Sr element may accelerate the electrochemical reaction occurred onto the alloys, resulting in deteriorated anti-corrosive properties. Furthermore, the behaviors of the alloys operated under different temperatures (Room temperature and 60 ºC) are also studied in this research, aiming to provide some useful guidance in alloy design and application.

Keywords: lead-acid battery; lead alloys; grids; corrosion properties

1. INTRODUCTION

Even the battery industries are very thriving with lots of new-typed batteries emerged, traditional lead-acid batteries (LABs) are still serving as important roles due to their low cost, reliable performance as well as safe property during operation [1-3]. The grid is one of the main components for LABs, which is responsible for electron transferring throughout the battery as well as holding the reactive substances. Therefore improving the grid performance, including improving its anti-corrosion properties, inhibiting the hydrogen and oxygen evolution, is very important for reducing the battery capacity decay, thus extending the service life of the batteries [4-8].

Pb-Sb alloys are first employed as the gird for lead-acid batteries in the first half of the 20th century. However, it is found in the 1950s that the Sb can aggravate the hydrogen evolution reaction during battery operation, making the Pb-Sb alloys cannot meet the requirements for maintenance-free lead-acid batteries [9-11], which has increased market share among all the lead-acid battery types during that period. In the 1970s, Pb-Ca alloys are widely investigated due to the higher hydrogen overpotential of Ca, while the superior mechanical property and high corrosion resistance help Pb-Ca alloys being the dominating grid candidate for lead-acid batteries [12-15]. However, some shortcomings are also found for Pb-Ca alloys while the formation of the intermetallic compound, Pb_3Ca crystals in the grain boundaries is claimed as the most severe one. The formed Pb_3Ca is easily suffering from oxidation in the battery operation process, resulting in intergranular corrosion of the grid bars and deterioration of the battery capacity [16]. Adding extra elements to the Pb-Ca grid is considered as the most effective strategy to solve this problem, while suitable additives are continuous searched during these years, such as Sn, Bi, Ag [17-22], which are tried as possible additive candidates and in-depth investigations are made on the obtained alloys.

Strontium (Sr) is also belong to alkaline earth metal (group IIA) and has similar chemical properties with Ca. However, the employment of Sr in lead-acid batteries and the detailed properties of Pb-Sr alloys have not been studied in detail to the best of our knowledge. Therefore, we prepared Pb-Sr alloys with different Sr content in this research, the physical, electrochemical, anti-corrosive properties of the obtained Pb-Sr alloys are studied in detail. For comparison, the properties of Pb-Ca alloys are also studied and provided.

Furthermore, the battery manufacturers have claimed that the working temperature range for lead-acid batteries are usually in the range from 40 ºC to 70 ºC, especially when the lead-acid batteries are engaged into the automotive operation. Thus investigations on the lead alloys under higher working temperature are pretty vital. Hence different temperatures are chosen in our study to gain some understandings on the alloy behaviors with varied temperatures, which is rarely focused on the previous papers.

2. EXPERIMENTAL PART

2.1. Preparation of the testing alloys

Pb-Ca and Pb-Sr binary alloys were processed by melting pure lead (99.99 wt.%), with different proportions of pure calcium (99.99 wt.%) or pure strontium (99.99 wt.%) together in the electrical furnace under an argon atmosphere at 1000 K for 15 min. Pouring the molten metal liquid into designed molds, collecting the alloys after cooling down to room temperature. The composition and sample ID of each alloy are listed in **Table 1**.

Table 1. Sample ID and the corresponding components of the alloys used in this study

Sample ID	Composition
Pb00	Pure Pb
C01	Pb-Ca (0.1 wt.% Ca)
C05	Pb-Ca (0.5 wt.% Ca)
S01	Pb-Sr (0.1 wt.% Sr)
S05	Pb-Sr (0.5 wt.% Sr)

There are two alloy types used in this study: one is a rod with a diameter of 8.0 mm and a length of 16 mm, this type of alloy was welded to the copper conductor and partially sealed with epoxy resin, the exposed surface of the rod was polished by metallographic sandpaper as the working electrode for electrochemical investigation; Another alloy type is a rectangular plate with dimensions of 20 mm×20 mm×2 mm, which is used in the corrosion testing. The microhardness of the alloy was measured using HMV-2T microhardness tester (Shimadzu instruments, Japan), and the applied pressure is 245.2 mN.

2.2. Electrochemical experiments

The electrochemical methods used in this paper are as follows: linear potential sweep (LSV), open circuit potential (OCP) and cyclic voltammograms (CV). Electrochemical tests were performed on a CH1660D electrochemical workstation (Shanghai chenhua instrument co., LTD） by using a three-electrode electrochemical system. The counter and reference electrodes were a platinum plate (4 cm^2) and Hg/Hg_2SO_4 electrode, respectively. All potentials reported in the paper are concerning this reference electrode. The electrolyte used was 1.28 g cm^{-3} sulfuric acid solution prepared by mixing the concentrated H_2SO_4 and double-distilled water. Before each electrochemical test, the working electrodes were mechanically polished with 1000 #, 2000 # and 4000 # SiC emery papers in sequence, and then rinse off the oil stains by anhydrous ethanol and double-distilled water. The electrochemical system was pre-reduction at a cathodic potential of -1.2 V for 10 min to eliminate the oxide formed on the surface of the alloys before each test, and all the electrochemical tests were performed at room temperature (RT) and 60 ºC, respectively.

2.3. Corrosion tests

Corrosion tests of the alloys were conducted in a simulated cell system, while pure lead plates and Pb-Ca or Pb-Sr plates connected in series alternately. The corrosion tests were carried out with a constant current of 10mA cm^{-2} at constant temperatures of RT and 60 ºC for 7 days, respectively. The electrodes before and after corrosion were weighed to calculate the corrosion rate. The morphology of the corrosion layers and corroded surfaces of each alloy were analyzed by using a scanning electron microscope (SEM, Phenom Pro X) and X-ray diffraction (Japan science instrument co. LTD).

2.4 Microstructure

The metallographic samples were prepared from the rod alloys, one end of which was mechanically polished by 1000#, 2000# and 4000# SiC emery papers. These samples were then chemically polished using a 1:1 (by volume) acetic acid/hydrogen peroxide solution, and etched with a solution containing 9 g of ammonium molybdate, and 15 g of citric acid in 90 g of distilled water. Then, the surfaces of alloys were washed with anhydrous ethanol and distilled water, respectively. The structure of the alloys was observed using a Nikon Eclipse 50i polarizing microscope (Nikon Corporation of Japan).

3. RESULTS AND DISCUSSION

3.1 Microstructure of alloys

The microstructure and microhardness properties of the alloys are shown in **Fig. 1**. When adding a small amount of Ca and Sr to the alloys, little effects on the microstructure of Pb alloys are found by comparing **Fig.1a**, **b**, and **d**. However, increasing the addition amount of both elements, the grain sizes in the alloys are reduced (**Fig. 1c** and **e**), resulting in larger hardness of the alloys accordingly as seen in panel f of **Fig. 1**. It's reported that this grain refinement is beneficial for preventing the recrystallization of the lead alloy and thus improve the structural stability, the smaller the grain size, the greater the hardness of the corresponding alloy[21,23-25]. As the carrier of active materials, the alloys are required to have a certain hardness in case of their easy deformation [26]. Compared with Pb-Ca alloys, Pb-Sr binary alloys with the same additive concentration exhibit lower hardness values, meaning that higher content of Sr may needed if it were used in the real industrial applications.

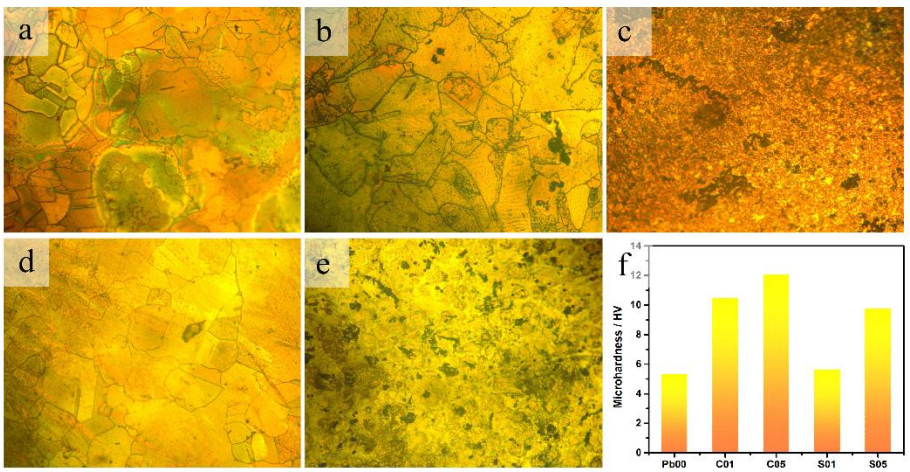

Figure 1. Optical micrographs of the samples: (a) Pb00, (b) C01, (c) C05, (d) S01, (e) S05 and (f) the microhardness of the alloys.

3.2 Hydrogen/oxygen evolution reaction (HER/OER) study

Hydrogen evolution reaction (HER) is a common phenomenon for metals, while the metals can act as catalysts to lower the energy needed in formation of H-H bond from water. HER on the gird affects the lead-acid battery life severely since water loss is one of the most significant battery failure mechanisms [27-28]. Therefore, hydrogen evolution potential being one important criterion to evaluate the performance of alloys. Besides, the hydrogen evolution kinetics can be reflected by the Tafel slope [23, 29], the *b* value as shown in equation 1.

$$\eta = a + b\ lgi \qquad (1)$$

To test the HER, linear potential sweep (LSV) technique was employed and a three-electrode configuration was used, the cathodic polarization curve was measured range a -1.2 V ~ -1.9 V potential with a sweep rate of 5 mV s^{-1} at 25 ºC and 60 ºC, respectively. The hydrogen evolution curves of the alloys and the corresponding kinetic parameter *b* calculated from the Tafel equation are shown in **Fig.2**. Adding Ca or Sr to the Pb matrix has similar effects on its hydrogen evolution properties at RT, that is, all the binary alloys exhibit better inhibition properties to HER, as shown in the cathodic polarization curves, while the *b* value shown in **Fig.2 c** and **f** also confirmed the reduced reaction kinetics for all the binary alloys. However, this behavior is changed when the operating temperature increased to 60 ºC, while the HERs seem much severe for the binary alloys compared with pure lead, especially for the Pb-Sr alloys. One possible reason is that the partial separation of Ca and Sr from the binary alloys under high-temperature operation, the separated Ca and Sr act as active sites for HER [30], resulting in higher reaction kinetics for hydrogen formation.

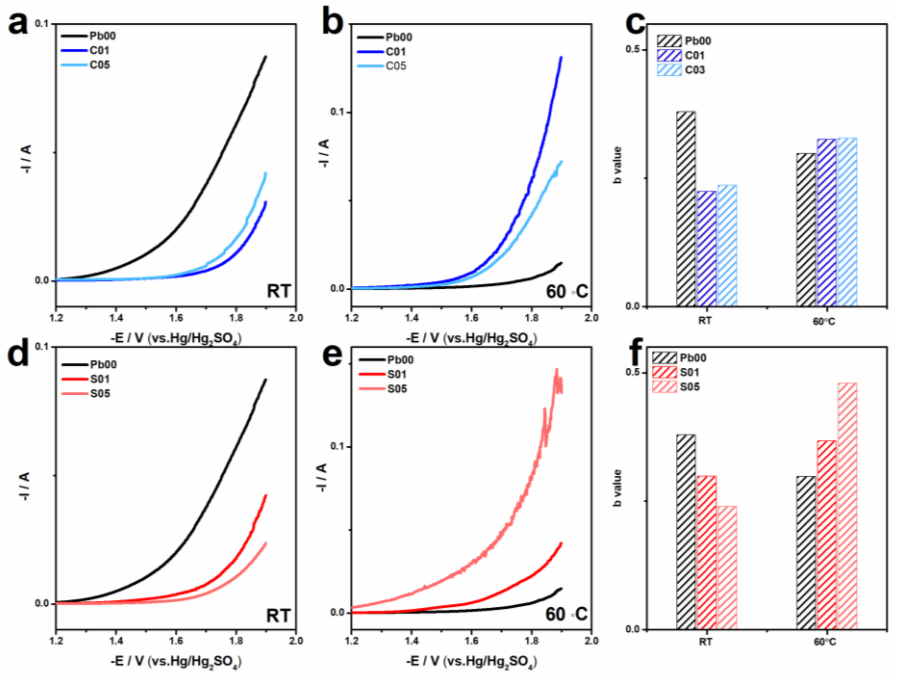

Figure 2. Hydrogen evolution reaction of Pb-Ca alloys at (a) RT and (b) 60 ºC, and HER of Pb-Sr alloys at (d) RT and (e) 60 ºC; The b value of (c) Pb-Ca alloys and (f) Pb-Sr alloys.

The oxygen evolution reaction (OER) on different alloys under RT and 60 ºC were also studied, and the results are shown in **Fig.3**. Before the LSV tests, the electrodes were pre-polarized at 1.7 V for 1 h in 1.28 g cm^{-3} H_2SO_4 solution to form an anodic layer of lead oxide [12,22-23]. Compared with HER, the OER behaviors for all the Pb-Ca and Pb-Sr alloys are similar and much closer reaction kinetics obtained from Tafel plots, whereas the OER on the binary alloys is also severer under higher temperature due to the similar reason for HER.

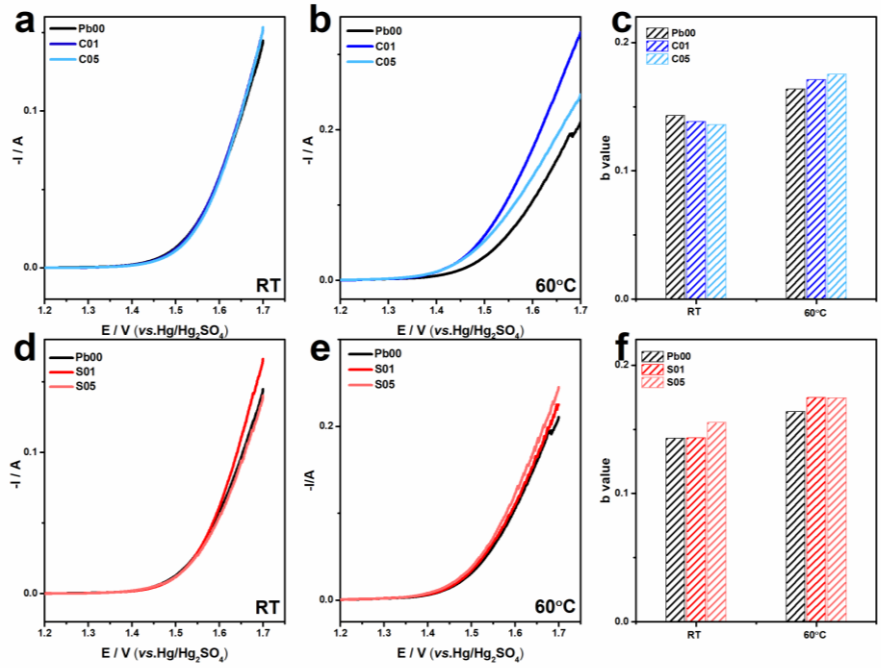

Figure 3. Oxygen evolution reaction of Pb-Ca alloys at (a) RT and (b) 60 ºC, and OER of Pb-Sr alloys at (d) RT and (e) 60 ºC; The b value of (c) Pb-Ca alloys and (f) Pb-Sr alloys.

3.3 The anti-corrosion property study under constant potential

1.3 V is the floating charge potential for lead-acid battery, so this potential was chosen to study the anti-corrosion properties of the alloys in this study. It is reported [21,31] that PbO_2 is mainly formed under this potential, thus the formation amount of PbO_2 can be used as a measurement index to evaluate the corrosion status of the alloys. The alloy electrodes were electrochemical oxidized at 1.3 V for 1 h to form PbO_2 film firstly, the formed PbO_2 will self-discharge with time prolonging. The potential changes with time were plotted and the results are shown in **Fig.4 a** and **b**. As can be seen, the potential decreased as time prolonging and a plateau, marked as AB, appeared at around 1.05 V. The length of AB can be an indicator to the PbO_2 amount. Among the different alloys, Pb-Ca (0.5 wt.%) exhibit apparently shortest length of AB, indicating the least PbO_2 formed on its surface, while the amount of PbO_2 increase with Ca concentration. On the contrary, the Pb-Sr binary alloys exhibit a much longer AB plateau, indicating much severe corrosion might be happened on this alloys when constant potential applied.

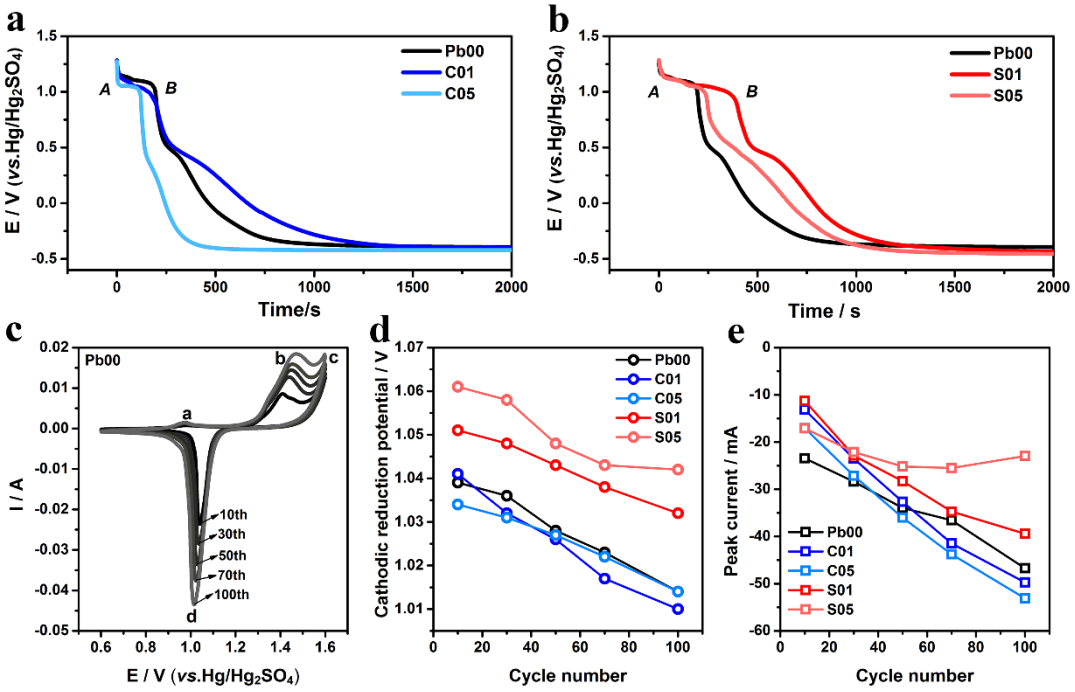

Figure 4. The anti-corrosion properties under constant potential: open circuit potential decay curves for (a) Pb-Ca and (b) Pb-Sr alloys, (c) the typical cyclic voltammetry, (d) the cathodic reduction potential and (e) peak current of different alloys

To further understand the electrochemical behavior of these alloys, cyclic voltammograms (CV) tests are performed onto the alloys in the range of 0.6~1.6 V at a sweep rate of 5 mV s^{-1}. **Fig.4** panel **c** exhibit a typical CV curves during this region: in the positive sweep, three anodic peaks: *a*, *b* and *c* are observed, corresponding to the oxidation of the Pb substrate to α-PbO_2, the transformation of $PbSO_4$ to β-PbO_2, and the evolution of oxygen, respectively; in the negative sweep, a cathodic peak *d* appeared, corresponding to the reduction of PbO_2 to $PbSO_4$ [6, 32]. We calculated the potential and the peak current change of peak *d* at 10^{th}, 30^{th}, 50^{th}, 70^{th}, and 100^{th}, and plot them in **Fig.4 d** and **e**. Clearly, the potential of peak *d* shifted to lower position with the cycle number increase, indicating ever-increasing polarization of the reaction due to the increased formation of porous reduction products onto the electrodes. Among all the alloys, it can be found the Pb-Sr (0.5 wt.%) alloy possess the highest cathodic reduction potential, meaning the least polarization it has among all the alloys, followed by the Pb-Sr (0.1 wt.%) alloy. It can be inferred that the Sr dopant can facilitate the electrochemical transformation reaction on the lead alloys, resulting in reduced reaction resistance. Besides, the peak current of Pb-Sr alloys also increased to a much higher value along with the cycling proceeding, indicating the highest reaction activity.

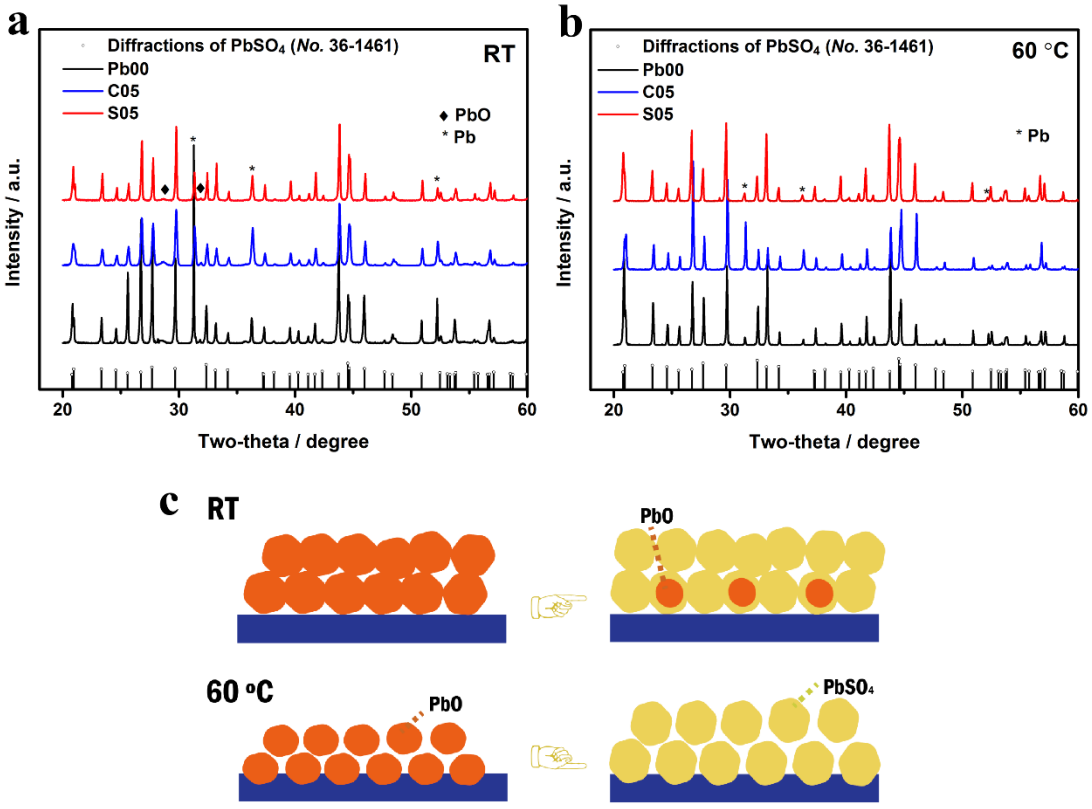

Figure 5. XRD pattern of the corrosion products formed on the alloys under constant current for one week: (a) alloys corroded at RT; (b) alloys corroded at 60ºC; (c) the possible corrosion mechanism.

3.4 The anti-corrosion property study under constant current

Anti-corrosion property of grid under constant current is vital as it effects the long-term cycling performance of lead-acid batteries [33-34], and we performed the corrosion tests for different lead alloys by assembling simulated cells as described in the experimental part, the corrosion tests were lasted for 7 days, under both RT and 60 ºC, with constant current applied.

The crystal structure of the corrosion products are studied by XRD, as shown in **Fig.5**, there are no distinct differences detected for Pb-Ca and Pb-Sr alloys possibly due to the low concentration of the additives. Most of the diffraction peaks can be well indexed by cubic $PbSO_4$ phase structure (PDF# 36-1461). Some extra peaks observed in the corrosive products obtained at RT (panel **a**, **c**) can be assigned to PbO (PDF# 05-0561), which cannot detected in the products obtained under high-temperature operation (**Fig.5 b**). Since the PbO cannot existed in acid environment, thus it can be reasonably inferred that the detected PbO should be the inner part of $PbSO_4$. The initial corrosion products, PbO, will further reacted with H_2SO_4 to form $PbSO_4$, while under lower temperature (RT), the resultant big-sized PbO crystals due to low corrosion rate cannot be fully reacted with H_2SO_4 before new PbO generated, resulting in incompletely reacted $PbSO_4$/PbO composites; on the contrary, the smaller and loosely packed particles formed under higher temperature will react with H_2SO_4 completely and thus no PbO can be detected. The possible mechanism is shown in **Fig.5** panel **c**.

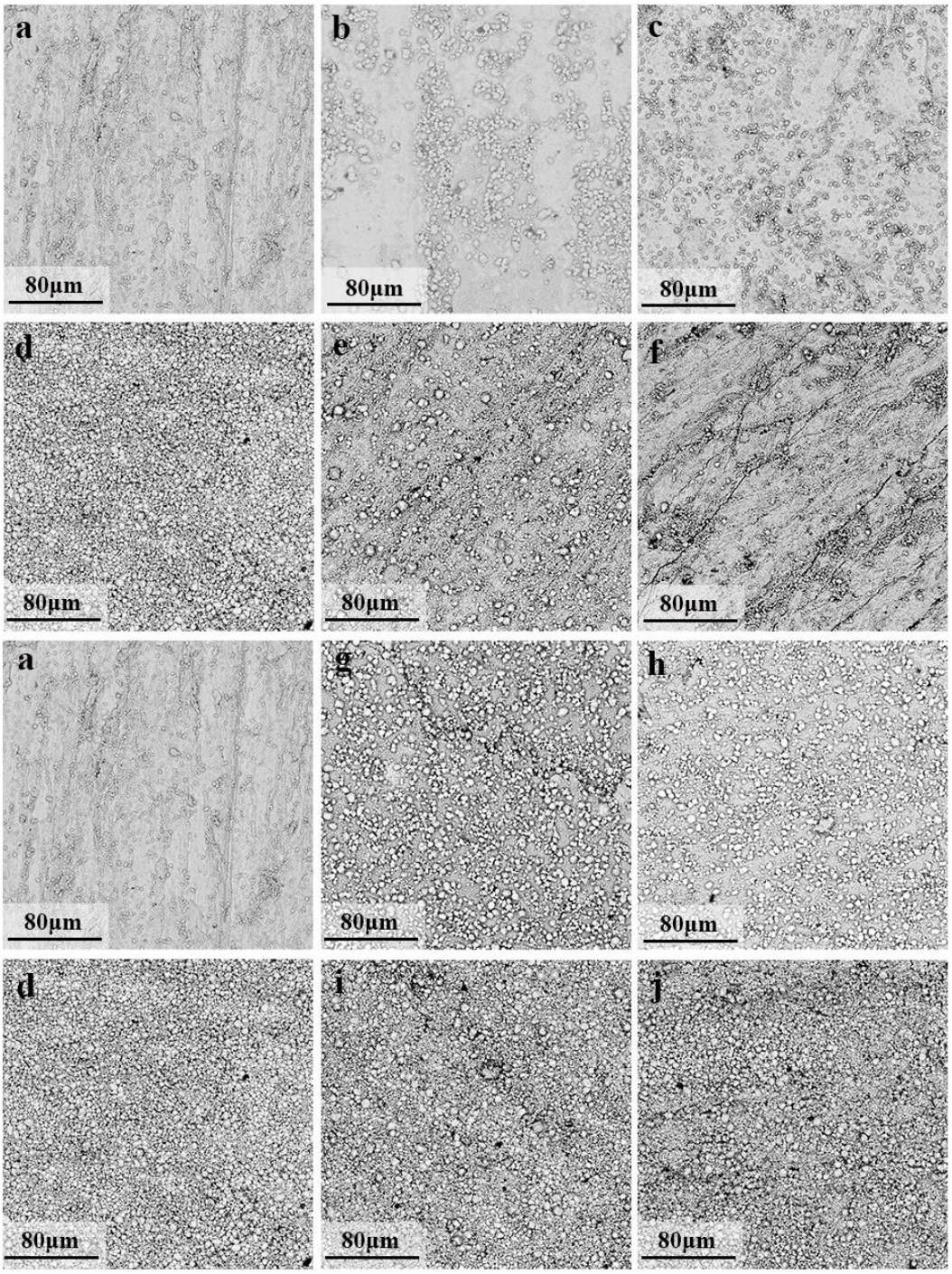

Figure 6. Morphology of the corroded alloys after wiping off the corrosion products: (a) Pb00 at RT, (b) C01 at RT, (c) C05 at RT, (d) Pb00 at 60 ºC, (e) C01 at 60ºC, (f) C05 at 60 ºC, (g) S01 at RT, (h) S05 at RT, (i) S01 at 60 ºC and (j) S05 at 60 ºC.

The morphology of the corroded grids after rinsing the corrosion products are studied by SEM, and the results are shown in **Fig.6**. Even we have already wiped out all the corrosion products formed on the alloys, some crystals are formed rapidly on the alloy surface before we perform SEM testing. These newly-formed crystals, as observed from the images, are mainly aggregated at the corroded cracks of the alloys, where have higher reactivity. That means more crystals gathered, more serious corrosion

of the alloys underwent. Based on this analysis, three main conclusions can be obtained according to **Fig.6**:

1) Pb-Ca alloys possess higher anti-corrosion properties compared with pure Pb and Pb-Sr alloys. The corrosion speed for different types of alloys under same condition increases in the order: Pb-Ca < Pure Pb < Pb-Sr.

2) Some cracks can be observed in the high-calcium binary alloys under high temperature (panel **f**), which should be ascribed to the high hardness of this alloy, meaning that Pb-Ca binary alloys with high-calcium is not proper to be used directly in the real industry field without further treatment, such as mixing with other elements.

3) All the lead alloys went through much serious corrosion under higher temperature.

4. CONCLUSION

Even the Sr has similar physical properties with Ca as they situated at the same group in the elemental periodic table, however, it exhibit completely different properties when used as dopant to pure lead alloys, as investigated in this study. We listed the conclusions obtained based on our study as follows:

1) Even the Sr can inhibit the HER to some extent, the inhibition effect cannot be maintained under higher working temperature, possible due to the partial dissolution of the additive, meanwhile, the Ca dopant also exhibit severer HER under higher temperature.

2) The Sr dopant can promote the electrochemical reaction onto the alloys by decreasing the reaction polarization, which is the possible reason for its deteriorated corrosion property under constant potential.

3) From the results of corrosion experiment under constant current, the Pb-Sr alloys also exhibit worst anti-corrosion properties as confirmed by SEM.

Besides, the electrochemical properties as well as the corrosion behavior seems different under higher temperature compared with RT, thus in order to meet the high-temperature demand of the alloys, some further strategies are needed to enhance their electrochemical properties.

ACKNOWLEDGEMENTS
This work was financial supported by the Science and Technology Program of State Grid Corporation of China (Program Name: Study on Positive Grid Alloy for Long Life Lead Carbon Batteries (DG71-17-009)).

References

1. K.R. Bullock, *J. Electrochem. Soc.*, 142 (1995) 1726.
2. M. Kniveton, *J. Power Sources*, 96 (2001) 140.
3. A.J. Li, Y.M. Chen, H.Y. Chen, D. Shu, W.S. Li, H. Wang, C.L. Dong, W. Zhang and S. Chen, *J. Power Sources*, 189 (2009) 1204.

4. A. Nuzhny, *J. Power Sources,* 158 (2006) 920.
5. R.K. Shervedani, A.Z. Isfahani, R. Khodavisy and A.H. Mehrjardi, *J. Power Sources,* 164 (2007) 890.
6. Y.B. Zhou, C.X. Yang, W.F. Zhou and H.T. Liu, *J. Alloys Compd.,* 365 (2004) 108.
7. G.F. Lin, G.S. Zhou, D.G. Li and M.S. Zheng, *J. Rare Earths,* 24 (2006) 232.
8. Y.B. Zhou, H.T. Liu, W.B. Cai, A.S. Wang and H.Y. Fan, *J. Electrochem. Soc.,* 151 (2004) 978.
9. N.E. Bagshaw, *J. Power Sources,* 53 (1995) 25.
10. T. Hirasawa, K. Sasaki, M. Taguchi and H. Kaneko, *J. Power Sources,* 85 (2000) 44.
11. M.P.J. Brennan, B.N. Stirrup and N.A. Hampson, *J. Appl. Electrochem.,* 4 (1974) 49.
12. S. Zhong, J. Wang, H.K. Liu and S.X. Dou, *J. Appl. Electrochem.,* 29 (1999) 1.
13. N.E. Bagshaw, *J. Power Sources,* 33 (1991) 3.
14. D.G. Li, G.S. Zhou, J. Zhang and M.S. Zheng, *Electrochim. Acta,* 52 (2007) 2146.
15. H. Giess, *J. Power Sources,* 53 (1995) 31.
16. D. Slavkov, B.S. Haran, B.N. Popov and F. Fleming, *J. Power Sources,* 112 (2002) 199.
17. H.Y. Chen, L. Wu, C. Ren, Q.Z. Luo, Z.H. Xie, X. Jiang, S.P. Zhu, Y.K. Xia and Y.R. Luo, *J. Power Sources,* 95 (2001) 108.
18. L.T. Lam, N.P. Haigh and D.A.J. Rand, *J. Power Sources,* 88 (2000) 11.
19. N. Bui, P. Mattesco, P. Simon, J. Steinmetz and E. Rocca, *J. Power Sources,* 67 (1997) 61.
20. P.H. Benhangi, D. Nakhaie, M.H. Moayed and A. Molazemi, *J. Power Sources,* 196 (2011) 10424.
21. W.X. Guo, D. Shu, H.Y. Chen, A.J. Li, H. Wang, G.M. Xiao, C.L. Duo, S.G. Peng, W.W. Wei, W. Zhang, H.W. Zhou and S. Chen, *J. Alloys Compd.,* 475 (2009) 102.
22. W.R. OsÓrio, C.S.C. Aoki and A. Garci, *J. Power Sources,* 185 (2008) 1471.
23. X.Y. Zhou, S. Wang, J. Yang, Z.C. Guo, J. Yang, C. Y. Ma and B.M. Chen, *Trans. Nonferrous Met. Soc. China,* 27 (2017) 2096.
24. H.X. Wu, F.R. Ai and H. Yan, *Acta Metall. Sini. (Engl. Lett.),* 25 (2012) 272.
25. Q. Liu, M.W. Liu, C. Xu, W.L. Xiao, H. Y, S.H. Xie and C.L. Ma, *Mater. Charact.,* 140 (2018) 290.
26. J. Wei, D.T. Wang, Z.H. Luan and Q. Guo, *J. Harbin Inst. Technol.,* 10 (2003) 28.
27. M. Maja, N. Penazzi, *J. Power Sources,* 22 (1988) 1.
28. J.H. Yan, W.S. Li and Q.Y. Zhan, *J. Power Sources,* 133 (2004) 135.
29. F. Wang, C. Hu, M. Zhou, K.L. Wang, J.L. Lian, J. Yan, S.J. Cheng and K. Jiang, *Mater. Sci.,* 61 (2016) 451.
30. W.S. Li, X.M. Long, J.H. Yan, J.M. Nan, H.Y. Chen and Y.M. Wu, *J. Power sources,* 158 (2006) 1096.
31. H.Y. Chen, S. Li, A.J. Li, D. Shu, W.S. Li, C.L. Dou, Q. Wang, G.M. Xiao, S.G. Peng, S. Chen, W. Zhang and H. Wang, *J. Power sources,* 168 (2007) 79.
32. W.F. Zhou, X.L. Cheng, *Acta Chim. Sin.,* 43 (1985) 333.
33. E. Rocca, G. Bourguignon and J. Steinmetz, *J. Power sources,* 161 (2006) 666.
34. P. Ruetschi, *J. Power Sources,* 127 (2004) 33.